Asian Journal of Pharmaceutical Sciences 13 (2018) 297–309

Available online at www.sciencedirect.com

ScienceDirect

journal homepage: www.elsevier.com/locate/AJPS

Original Research Paper

Novel technique of insulin loading into porous carriers for oral delivery☆

Sarah Y. Eilleia, Mahmoud E. Soliman, Samar Mansour, Ahmed. S. Geneidi*

Department of Pharmaceutics and Industrial Pharmacy, Faculty of Pharmacy, Ain Shams University, Cairo 11566, Egypt

ARTICLE INFO

Article history:
Received 24 August 2017
Revised 29 December 2017
Accepted 16 March 2018
Available online 17 April 2018

Keywords:
Porous microparticles
PLGA
Insulin
Freeze-drying
Chitosan coating

ABSTRACT

The increasing demand for oral macromolecule delivery encouraged the development of microencapsulation technologies to protect such drugs against gastric and enzymatic degradation. However, microencapsulation often requires harsh conditions that may jeopardize their biological activity. Accordingly, many trials attempted to load macromolecules into porous drug carriers to bypass any formulation induced instability. In this study, we prepared chitosan coated porous poly (d, l-lactide-co-glycolide) (PLGA) microparticles (MPs) loaded with insulin using a novel loading technique; double freeze-drying. The results showed a significant increase in drug loading using only 5 mg/ml initial insulin concentration and conveyed a sustained drug release over uncoated MPs. Furthermore, SEM and confocal microscopy confirmed pore blocking and insulin accumulation within the MPs respectively. The oral pharmacodynamic data on rats also proved the preservation of insulin bioactivity after formulation. Finally, the new coating technique proved to be efficient in producing robust layer of chitosan with higher insulin loading while maintaining insulin activity.

1. Introduction

Recent achievements in biotechnology promoted the development of many therapeutic macromolecules, such as synthetic gonadotropin-releasing hormone analog (Goserelin) [1], glucagon-like peptide-1 (GLP-1) [2] and insulin. Despite the selectivity and efficiency of such molecules, they are commonly administered through injection. The major drawback with needle injections is the patient compliance, especially with chronic diseases such as diabetes mellitus. Despite the numerous trials performed to deliver therapeutic macromolecules molecules through alternative routes as pulmonary [3] or transdermal [4] oral route remains the most convenient way [5] not only because of the ease of administration but also because it mimics the normal physiological

☆ Peer review under responsibility of Shenyang Pharmaceutical University.

* Corresponding author. Department of Pharmaceutics and Industrial Pharmacy, Faculty of Pharmacy, Ain Shams University, Cairo 11566, Egypt. Tel.: +2 0106503814
E-mail address: Sarah.youssef@pharma.asu.edu.eg (S.Y. Eilleia).

https://doi.org/10.1016/j.ajps.2018.03.003

pathway of insulin where it goes to the liver via the portal vein after absorption from the gastro intestinal tract (GIT) [6]. However, the oral delivery of insulin or any other therapeutic proteins faces several challenges because of the complicated physiology of the GIT in terms of gastric acidic environment, enzymatic degradation and difficulty of absorption of large polar molecules [7]. The previously stated challenges have led to the utilization of polymer microencapsulation techniques in order to protect macromolecules from degradation in the GIT. [5]. The most common microencapsulation techniques involve the use of organic solvents that may lead to the exposure of hidden hydrophobic fractions of macromolecules at the organic/aqueous interface and subsequently causes structure denaturation [8,9,10]. As a consequence, many researchers have tried to overcome these formulation problems by fabricating porous particles and loading the macromolecules inside the pores. For instance, Puri et al. examined the release of bovine serum albumin and dextran adsorbed into porous PLGA MPs where they studied the effect of protein/polymer interaction on the release rate [11]. Porous polymeric MPs are usually synthesized by solvent emulsion technique which produces large polydisperse macropores [12].

Nevertheless, the main problem with conventional adsorption techniques is that the loading capacity is minimal for most molecules and requires high initial loading amount of protein, whereas the cargo release can be very fast from the pores [13]. These drawbacks are the reason why researchers developed different techniques that can be used for pore blocking after drug loading, aiming to increase protein loading and sustain its release. [14]. For instance, Reinhold et al. [15] and Bailey et al. [16] were able to block the pores of polymeric PLGA MPs using heat for 30–48 h. Other groups studied pore closure after loading of their cargo onto preformed porous PLGA MPs by immersing them in organic solvents as acetonitrile [14] or hexane [8] and could maintain a sustained release pattern over 72 h. However, the use of either heat or organic solvents may lead to a premature release of the cargo molecules. Additionally, these methods might disrupt the structural integrity of the carrier vehicles and they can cause damage to the sensitive drug molecules. In the GIT, these particles may be also washed out before drug release and possible absorption by enteric epithelium [5]. Eventually, polymer coating was chosen to be an optimum solution in ways of both blocking the pores and suitability for oral administration [17]. However, the effect of polymer coated post-loaded porous MPs on oral administration was hardly examined [18,19].

Several polymers were employed in coating PLGA MPs; alginate [20], poly ethylene glycol [17], polymethacrylic acid [21] or chitosan. Of all these polymers, chitosan (CS) is by far the most common polymer used in MP coating because of its biocompatibility, mucoadhesion and penetration enhancing property [22].

Herein, we used porous MPs made of PLGA for examining the effect of chitosan coating on the loading and the release of insulin from macropores. For the facile adsorption of insulin a novel technique was used. To the best of our knowledge, the so-called double freeze-drying technique has not been employed so far for something similar.

2. Materials and methods

2.1. Materials

Poly-DL (lactide co-glycolide) 50:50; with molecular weight (Mwt) (15 kDa) (kindly supplied by Corbion Purac biomaterials, Netherlands), human insulin (Biocon, India, supplied by Sedico pharmaceuticals, Egypt), chitosan low and high Mwt (70 and 350 kDa, viscosity 9 and 16 cP respectively, degree of deacetylation > 85%) (Primex Ehf, Iceland), polyvinyl alcohol (PVA) Mwt 31–50 000 (Sigma Aldrich, USA), fluorescein isothiocyanate (FITC) (Sigma Aldrich, USA), streptozotocin (STZ, ≥98%) (Sigma Aldrich, USA), β-hydroxypropyl cyclodextrin (HPβCD) (Fluka, Germany), acetonitrile HPLC grade ≥ 99.9% (Fluka, Germany), methylene chloride (DCM, >99%, HPLC grade) (Tedia, India), dimethylsulfoxide (DMSO, >99%) (Tedia, India), acetic acid, ≥99%, (Sigma Aldrich, USA), deionized water (DI) from Milli-Q^{TM} water purification system (Millipore, USA). Other reagents, potassium dihydrogen phosphate, sodium phosphate dibasic anhydrous, sodium hydroxide, ammonium chloride, sodium bicarbonate, sodium carbonate, tri sodium citrate and citric acid anhydrous (analytical grade) were all purchased from El Nasr pharmaceutical company, Egypt.

2.2. Preparation of porous PLGA microparticles

PLGA MPs were synthesized using a water in oil in water (W/O/W) emulsion solvent evaporation method [3]. The primary emulsion was prepared by adding HPβCD to 0.6 ml 5% PVA, followed by emulsification with 250 mg PLGA in DCM (2 ml) and homogenization at 16,000 rpm for 2 min using a Heidolph Diax 900 homogenizer, Germany. The primary emulsion was poured onto 1% PVA solution (75 ml) and homogenized for another 3 min. The MPs were magnetically stirred overnight, then washed three times with DI and lyophilized using Christ alpha 1–2 LD plus lyophilizer (Christ, Germany).

2.3. Preparation of chitosan coated insulin loaded MPs

Surface coating of MP samples with chitosan: 10 mg porous PLGA MPs were incubated with an insulin solution 5 mg/ml in 0.01 M HCl (1 ml). The suspension was stirred for 4 h at 4 °C in dark, then lyophilized overnight. The freeze-drying cycle involved freezing at −50 °C, followed by the sublimation of frozen water at 0.065 mbar vacuum till complete dryness after 16 h. The MP/insulin mixture was reconstituted in chitosan solution (2.5, 5, 10 and 15 mg/ml) (1 ml) in 0.1 M acetate buffer pH 4 and stirred for another 4 h before entering a second freeze-drying cycle. 1 ml chitosan solution (5 mg/ml) containing insulin (5 mg) was stirred with MPs overnight or lyophilized once to test the effect of absent, single or double freeze-drying on insulin loading.

2.4. Characterization of porous MPs

Laser diffraction method was used to determine particle size. The dried MP samples were suspended in distilled water and

the obtained homogenous suspensions were examined to determine the mean diameter and span index which was used as an indicator for MP size polydispersity.

The porous morphology of MPs before and after CS coating was visualized using scanning electron microscopy (JEOL 5500, Tokyo, Japan). First, the MPs were gold sputtered for 1 min (Spi sputter coater, Westchester, USA). The MPs were fixed on a metal slab using a double adhesive tape. Pore diameter of PLGA MPs was quantified using image analysis software of a quanta FEG 250 scanning electron microscope. Since surface porosity is important indication for drug loading, we performed surface porosity analysis similar to what reported in [23] with slight difference using the sum of total surface area of pores instead of using area fraction.

The surface porosity values obtained represent the percentage of surface pore area per unit area (1 μm^2) of PLGA MPs as follows:

$$\text{Surface porosity \%} = \Sigma\left(\frac{\text{sum of pore areas}}{\text{MP surface area}}\right) \Big/ 50 \times 100 \quad (1)$$

2.5. Determination of insulin loading capacity

Lyophilized samples were redispersed in 1 ml DI, then centrifuged for 8 min at 13 680 rcf/12 000 rpm at 4 °C using Hermle z111 cooling centrifuge, (Hermle, Germany). The supernatant was removed and the MPs were washed with 100 µl DI to remove any excess peptide on the MP surface then the loaded insulin was extracted by adding a mixture of 1 ml 0.05 M HCl/0.4 ml acetonitrile according to [3]. The extracted insulin was determined using a Shimadzu UV-1601 PC spectrophotometer (Shimadzu, Japan)

The loading capacity (LC%) was calculated according to the following equation:

$$\text{LC\%} = \left(\frac{\text{insulin in MPs}}{\text{wt of the particles}}\right) \times 100 \quad (2)$$

2.6. Synthesis of fluorescein isothiocyanate conjugates with insulin (I-FITC)

Conjugation of FITC to insulin was done according to a method previously described in the literature [24]. 8 mg FITC was dissolved in 1 ml DMSO, yielding a final concentration of 2 mM. 250 µl of the FITC stock solution was added in 5 µl aliquots to 40 mg of an insulin solution (1.4 mM), dissolved in 5 ml carbonate buffer at pH 9. The reaction mixture was stirred for 2 h in the dark, before 250 µl of a 1 M NH_4Cl solution was added to quench excess fluorescence. Excess dye was removed using a PD-10 gel filtration column (GE healthcare, UK). The F/P ratio (1.5) was determined from the absorbance of the peptide and FITC at 277 and 495 nm respectively [24]. The I-FITC conjugate was used in further studies to examine the distribution of insulin in MPs and to study the insulin release pattern from MPs.

2.7. Determination of I-FITC distribution in coated MPs

In order to visualize the insulin distribution within the MPs before and after CS coating, confocal imaging was used to examine I-FITC loaded MPs [15,25]. MPs were re-dispersed in DI placed on a glass slide and covered with a cover slip. The particles were then imaged at excitation and emission wavelengths of 495 and 517 nm respectively using confocal microscope (Zeiss CLSM 710, Carl Zeiss, Germany). MP samples were scanned to a depth of 20 µm by a 1 µm increment using a 63x objective length in a z-stack mode. Finally images were processed using LSM image browser software 4.2.

2.8. In vitro release of I-FITC from porous MPs

The release of insulin from both coated and uncoated MPs were studied at pH 7.2. 1 ml I-FITC (insulin concentration corresponding to 5 mg/ml in carbonate buffer pH 9) was acidified to pH 3 with 2 M HCl then loaded into the pores of the particles. Subsequently, the MPs were coated with CS as mentioned in CS coating section. Afterward, 10 mg of CS coated PLGA MPs was redispersed in 1 ml DI, centrifuged for 8 min at 12 000 rpm at 4 °C. The supernatant was removed, the particles were washed with 100 µl DI and suspended in 4 ml phosphate buffer pH 7.2 then placed in a shaking water bath at 37 °C. 3 ml of the particle suspension was centrifuged at each time interval and replaced with a fresh buffer solution. I-FITC concentration was determined using an LS50 B spectroflourimeter (Perkin-Elmer Instruments, USA) at excitation and emission wavelengths of 474 and 504 nm respectively. In order to simulate the effect of pH variation in GIT on insulin release from chitosan coated MPs, I-FITC loaded CS-PLGA MPs were released in two different release media at pH values of 7.2 and 1.2. All aliquots were diluted and measured in pH 7.2.

2.9. Determination of insulin structural stability using sodium dodecyl sulfate polyacrylamide gel electrophoresis (SDS-PAGE)

In order to trigger detect the cargo integrity after loading, the insulin-loaded MPs were extracted using 0.01 M HCl for 12 h in a water bath adjusted at 37 °C. The samples were boiled for 5 min with 2% SDS and 10 mM β-mercaptoethanol in tris-glycine buffer pH 7.5, then run along a 16% SDS polyacrylamide gel for 4 h at 200 V before it was stained with Comassie Blue [26,27,28].

2.10. Determination of protein integrity using spectrofluorimetry

The tertiary structure of insulin was determined using fluorescence spectrophotometer at excitation and emission wavelengths 277 and 307 nm respectively. The fluorescence spectrum was compared to standard insulin in 0.01 M HCl (1 mg/ml) and denatured insulin sample which was left in a water bath for a month at 37 °C.

2.11. In vivo experiments

2.11.1. Animals

For studying the effect of insulin released from MPs on lowering blood glucose, Sprague–Dawley male rats (170–200 g) were kept for a week before experiment under 12 h day/night cycle at room temperature. Each rat was intraperitoneally injected

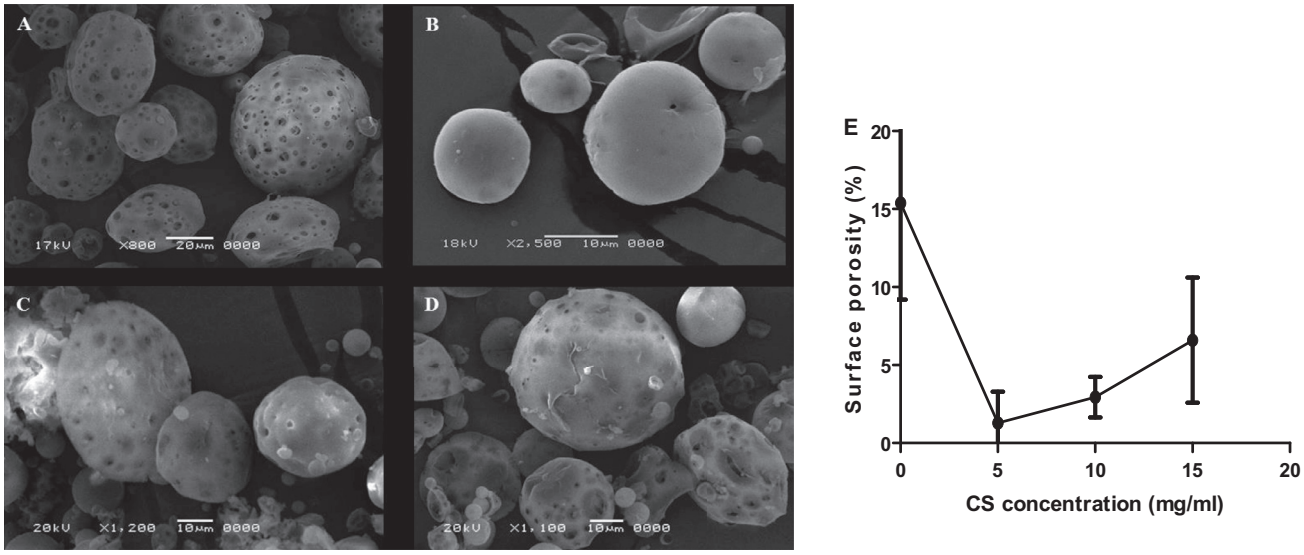

Fig. 1 – Scanning electron micrographs of (A) porous PLGA MPs, (B) CS-PLGA MPs concentration 5 mg/ml, (C) CS-PLGA MPs concentration 10 mg/ml, (D) CS-PLGA MPs concentration 15 mg/ml, (E) Effect of CS concentration on surface porosity of PLGA MPs as calculated from SEM images.

with STZ in a dose of 60 mg/kg dissolved in a sterile 0.1 M citrate buffer pH 4.5. The blood glucose level was monitored till diabetes induction. In five days, rats were considered diabetic if their plasma glucose level exceeded 200 mg/dl. All animal handling agreed with the guidelines of the ethical committee at the Faculty of Pharmacy Ain Shams University, Cairo, Egypt.

2.11.2. *Oral administration*

For the pharmacodynamics experiment diabetic rats were fasted for 12 h and divided into four groups (5 animals each) with free access to water. Group I was used as positive control and administered insulin injection subcutaneously (SC) at a dose of 5 IU/kg (0.18 mg/kg). Groups II-IV administered insulin loaded PLGA MPs, insulin loaded CS-PLGA MPs and oral insulin suspension (negative control) in doses equivalent to 50 IU/kg (1.8 mg/kg). At each time interval 0.5, 1, 2, 3, 4, 6, 8, 10 h, blood glucose was measured with using Accu-Chek® monitoring kit (Roche Diagnostics, USA) and the mean blood glucose reduction ± standard error of the mean (SE) was plotted against time. The area above the curve (AAC) was calculated in order to determine the relative bioavailability (BA_{rel}) compared to subcutaneous injection [5] using the following equation

$$BArel = \left(\frac{AAC_{oral} \times Dose_{SC}}{AAC_{SC} \times Dose_{oral}}\right) \times 100\% \quad (3)$$

2.12. *Statistical analysis*

All measurements were performed in triplicates, and the mean value ± standard deviation was calculated unless otherwise stated. Significance was determined using analysis of variance (ANOVA) tests. Data was considered significant when P value was <0.05.

3. Results and discussion

3.1. *Preparation of porous MPs*

Porous PLGA MPs were prepared by modified w/o/w emulsion technique where HPβCD was used as an osmotic agent and incorporated in the primary aqueous phase to increase the osmotic pressure relative to that of the external phase. Pores would be formed from leaching of osmogen during secondary emulsion formation. As shown in Fig. 1A, this method created large porous surface with high degree of polydispersity of pore diameter ranging from 0.5 to 5 μm. The polydispersity of pore diameter is a result of the heterogeneous energy introduced from high shear homogenization affecting the speed of polymer precipitation during particle formation and hence pore formation [29].

According to Ungaro et al., the increase in osmotic porogen concentration in porous PLGA formulation in turn increases the osmotic pressure leading to a higher degree of porosity [12]. However our SEM data indicated that these findings can only be applied up to a certain concentration. In our case, three concentrations of HPβCD (5%, 10% and 20%w/w) were examined for their porosities by SEM visual analysis software (Fig. 2).

Surface porosity of PLGA MPs increased from 1.15% ± 0.3% to 2.43% ± 0.7% when HPβCD concentration was raised from 5% to 10%, however, further increase in HPβCD concentration produced MPs with almost no number of surface pores. It can be hypothesized that increasing HPβCD concentration above specific level can increase the probability of forming a complex with PVA and hinders the leaching of the porogen from the MP matrix to form pores. Therefore, HPβCD concentration 10% (w/w) was selected for further studies as it would provide a highly porous structure that can accommodate more peptide.

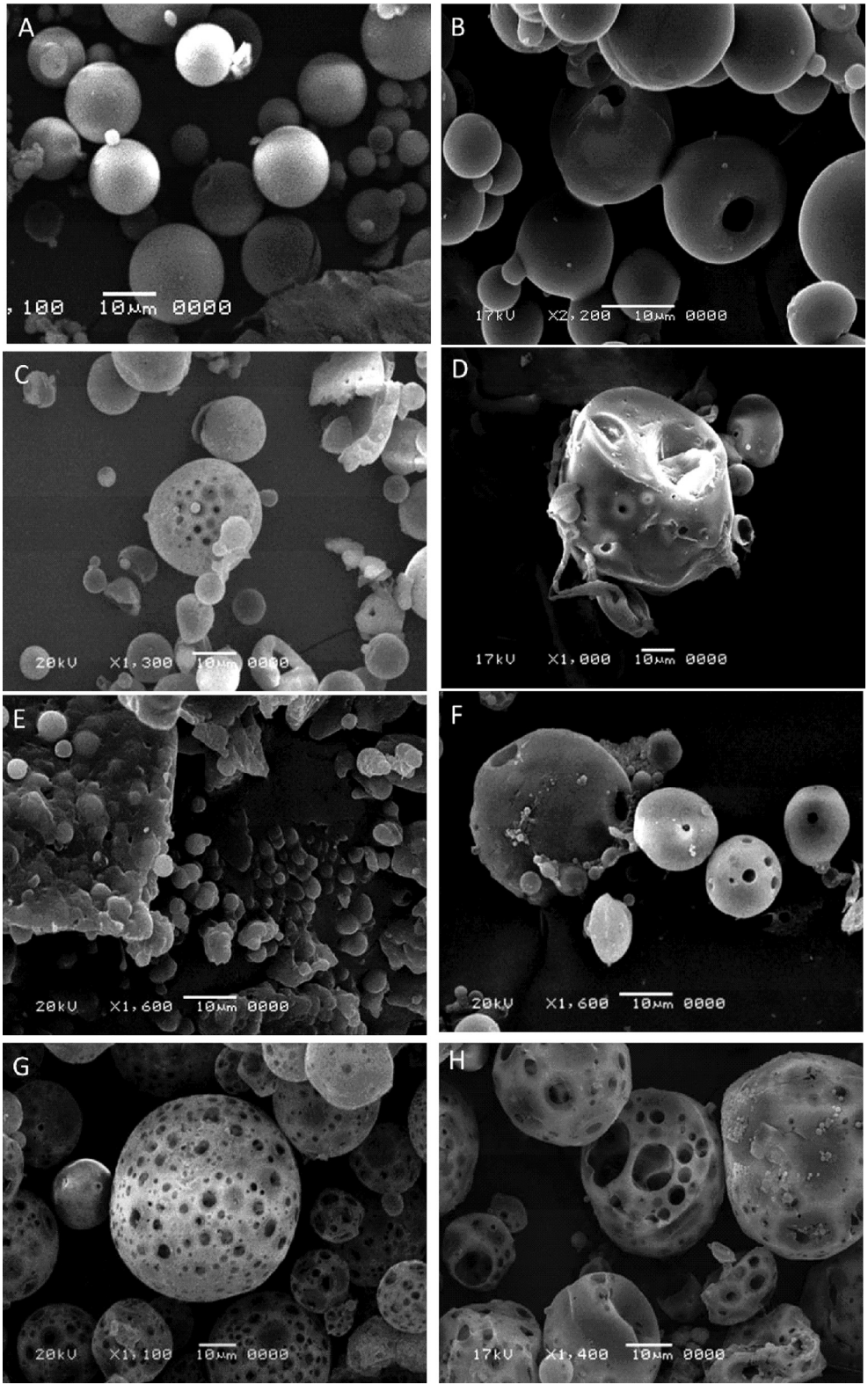

Fig. 2 – SEM micrographs of (A) plain non-porous PLGA MPs prepared from PLGA 7 kDa without adding any porogens, (B) plain porous PLGA MPs prepared with HPβCD 5% (w/w) and PLGA 7 kDa (C) plain porous PLGA MPs prepared with HPβCD 10% (w/w) and PLGA 7 kDa outer porous morphology and (D) cut section showing the inner porosity of the MPs in Fig. 2C, (E) plain porous PLGA MPs prepared with HPβCD 20% (w/w) and PLGA 7 kDa (F) plain porous PLGA MPs prepared with HPβCD 10% (w/w) and PLGA 15 kDa showing outer porous morphology and (G) cut section showing the inner porosity of the MPs in Fig. 2F (H) plain porous PLGA MPs prepared with HPβCD 10% (w/w) and PLGA 80 kDa.

Table 1 – Determination of surface porosity parameters for different plain PLGA formulae.

*PLGA M wt. (kDa)	HPβCD concentration (% w/w)	MP diameter ± SD (μm)	Span index ± SD	*Surface porosity ± SD (%)	Pore diameter ± SD
7		16.1 ± 0.3	1.2 ± 0.01		
7	10	17.2 ± 0.6	1.3 ± 0.01	2.4 ± 0.7	2 ± 1.5
15	10	29.4 ± 0.1	1.4 ± 0.01	15 ± 6	2.5 ± 1.3
80	10	57.4 ± 0.8	2.6 ± 0.2	3.7 ± 2.4	1.7 ± 1.4
7	5	13.4 ± 4.5	2 ± 0.04	5.1 ± 3.1	3.8 ± 1.1
7	20				

Data is represented as mean ± SD, n = 3.

The effect of PLGA Mwt on surface porosity was also examined using three different Mwts (7, 15, 80 KDa) of the polymer. By visual inspection and surface porosity data (Table 1), it can be noticed that surface and bulk pores significantly increased from 2.4% ± 0.7% to 15.4% ± 6% ($P < 0.001$), with increasing Mwt from 7 to 15 kDa but by further increase in Mwt, MP porosity decreased again to 2.8% ± 2.3%. This may be due to the fact that the higher the Mwt of PLGA, the faster the polymer precipitation forming solid polymer-shell during MP premature stages. Consequently, porogen premature escape will be minimal as the polymer precipitates and the porogen can be held within the polymer matrix, afterward, porogen extraction to the external aqueous phase can be achieved and the MPs will be more porous due to the defects produced during the escape of porogen through the formed viscous shell [30]. However, with further increase in Mwt from 15 to 80 kDa the polymer solution becomes too viscous for the porogen to be extracted in the external water phase leading to the formation of MPs with lower porosity [29]. In all formulations both pore diameters and pore diameter distribution were not significantly affected by either PLGA Mwt or HPβCD concentration but rather the density of surface pores was significantly affected by both parameters. It is also clear that increasing the polymer Mwt had a direct relation to MP size and span index ($P < 0.001$); reaching up to 40 ± 20 μm with the highest PLGA Mwt. From the data above, we used HPβCD concentration of 10% (w/w) and polymer Mwt of 15 kDa for further investigations.

3.2. *Factors affecting insulin loading efficiency*

3.2.1. *CS molecular weight*

Two different CS Mwts (low, high) were used to coat PLGA MPs with double freeze-drying technique. Fig. 3A shows that low Mwt CS had significantly ($P < 0.001$) higher LC% at CS concentrations 5 and 10 mg/ml and slightly higher values at the other concentrations (2.5 and 15 mg/ml).

3.2.2. *CS concentration*

Different concentrations of CS were tested to choose the optimum amount of CS to coat the particles without inducing aggregation or reducing drug loading efficiency. When studying the effect of various concentrations of both low and high Mwt CS on insulin LC% with PLGA MPs (Table 2), it was found that insulin LC% significantly increased ($P < 0.05$) as the concentration of CS increased. It reached a LC% value of 20% ± 0.9% at CS concentration 5 mg/ml, after which this finding was reversed and the LC% decreased to 6.9% ± 0.9% and 3.6% ± 0.3% at CS concentration of 10 and 15 mg/ml respectively.

A possible explanation could be that at low concentrations, the polymer chain can be desorbed upon re-dispersion leading to premature drug release. As the CS concentration increases, the polymer chains swirl taking a 'train/loop' conformation [29]. This conformation increases the effective contact area with MPs as they fill the pores. Consequently the viscosity of the coating layer increases preventing insulin leaching out of the pores during the reconstitution step. Further increase in

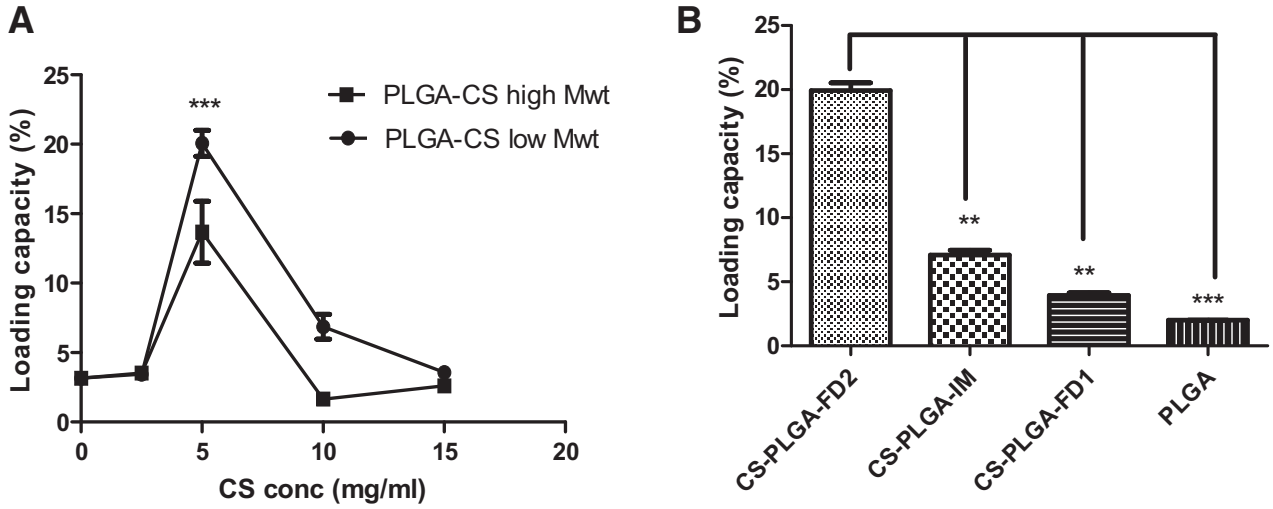

Fig. 3 – (A) Effect of CS concentration and molecular weight on insulin loading capacity using double freeze-drying technique onto CS-PLGA MPs, n = 3, (*) significant difference from uncoated particles, $P < 0.05$. (B) The effect of different coating techniques on insulin capacity on CS-PLGA MPs with CS concentration 5 mg/ml, n = 3, (*) significance among PLGA samples, $P < 0.05$.

Table 2 – The effect of CS molecular weight and concentration on insulin LC% from PLGA MPs using double freeze-drying technique.

M wt. of CS	Concentration of CS (mg/ml)	LC ± SD (%)
—	0	2 ± 0.02
Low	2.5	3.5 ± 0.4
Low	5	20.1 ± 0.9
Low	10	6.9 ± 0.9
Low	15	3.6 ± 0.3
High	2.5	3.5 ± 0.4
High	5	13.7 ± 2.2
High	10	1.7 ± 0.3
High	15	2.6 ± 0.4

Data is represented as mean ± SD, n = 3.

Table 3 – The effect of CS loading methods; immersion (IM), freeze-drying (FD1) and double freeze-drying (FD2) on insulin LC% at CS concentration (5 mg/ml).

Loading technique	LC ± SD (%)
IM	5.4 ± 2
FD1	3.9 ± 0.2
FD2	20.1 ± 0.9

Data is represented as mean ± SD, n = 3.

CS concentration and similarly Mwt, causes an increase in the viscosity which drive deposition of higher amounts of polymer chains on the initial layers. As a result, the deposited layers become loose due to the repulsion between the cationic CS chains and would be easily leached upon reconstitution taking the insulin payload with it [29].

3.2.3. *Coating method*

In order to confirm the effectiveness of double freeze-drying technique on increasing LC%, passive coating was done where a mixture of insulin and CS was incubated with PLGA MPs overnight or freeze-dried in a single step. As seen in Fig. 3B, double freeze-drying showed significantly ($P < 0.01$) higher values of LC% of PLGA formulae prepared by double freeze-drying in comparison to MPs loaded by simple mixing or single freeze-drying. An explanation for this might be that the CS layers initially adsorbed on the surface would hinder further penetration of relatively small insulin molecules into deeper pore structure inside the particles but instead remain only captured within the coating layer in the surface pores (Table 3) [31].

3.3. *Insulin loading and chitosan coating of porous MPs*

Coating of insulin loaded porous MPs with CS was investigated in an attempt to increase the loading and sustain the release of insulin by blocking surface pores. CS was selected because it is a biocompatible polymer well known for its capability of opening tight junctions between epithelial cell lining of GIT [32] as well as its adhesive properties to mucus layer secreted by gut wall [33]. For this reason, CS is considered one of the most suitable polymers for oral preparations [34,35]. The most common techniques of coating PLGA with CS involved the addition of CS in the secondary emulsion phase during the formation of PLGA MPs via emulsion solvent evaporation method [36]. Coating would be formed by either electrostatic or covalent bonds between CS and PLGA surface during MP formation [37]. However, this technique would not be feasible with post-loading of macromolecules. Hence, other research groups performed CS coating by incubating the polymer with drug loaded MPs known as "immersion technique" [38,39].

The mechanism of CS adsorption onto the surface of PLGA was known to follow Freundlich isotherm indicating multilayer adsorption [29]. It has been also reported that CS/PLGA interactions depend on hydrophobic or electrostatic interaction between positively charged chitosan and carboxyl end groups on the PLGA surface [38]. Since passive incubation with CS solution could risk the loss of pre-adsorbed drug especially from large pores of PLGA MPs, we developed a new technique based on double freeze-drying. In this method, the preformed MPs were loaded with insulin by freeze-drying and CS coating was then performed by re-suspending the MPs in chitosan solution using a second freeze-drying cycle. After reconstitution in CS solution, the excess insulin remaining after the first freeze-drying cycle would not only aid in suppressing insulin desorption by the effect of concentration gradient but would also help increasing the amount of insulin loaded into the MPs.

Coating by freeze-drying is a combination between two conventional techniques, namely, freezing and vacuum drying. The theory behind freezing lies in the difference in freezing points of water inside the pores of the substrate MPs and that in the bulk. Such difference, accounts for the super-cooled state inside the pores leading to an influx of solutes along with a vapor pressure gradient between bulk ice layer and the liquid water state remaining in the pores [40,41]. Similarly, the sublimation of solvent by vacuum increases the concentration of the solution and more solutes can accumulate inside the pores due to the variation in surface tension leading to stronger capillarity [42,43]. Hence, the use of both physical phenomena augmented the adsorption of both small insulin molecules and large CS chains into porous MPs.

3.4. *Morphological characterization of CS coated MPs*

CS coated PLGA formulae were visualized using SEM. SEM micrographs (Fig. 1B–D) show the deposition of CS onto the

Table 4 – The effect of selected CS molecular weight and concentration on surface porosity % for plain PLGA MPs using double freeze-drying technique.

M wt. of CS	Concentration of CS (mg/ml)	Surface porosity % ± SD(%)	MP diameter (μm) ± SD	Span index ± SD
—	0	15 ± 6	29.4 ± 0.1	1.4 ± 0.01
Low	5	1.3 ± 0.02	29.5 ± 2	1.8 ± 0.01
Low	10	2.9 ± 1.3	29.9 ± 4	2 ± 0.01
Low	15	6.6 ± 4	30.4 ± 4	2 ± 0.01

Data is represented as mean ± SD, n = 3.

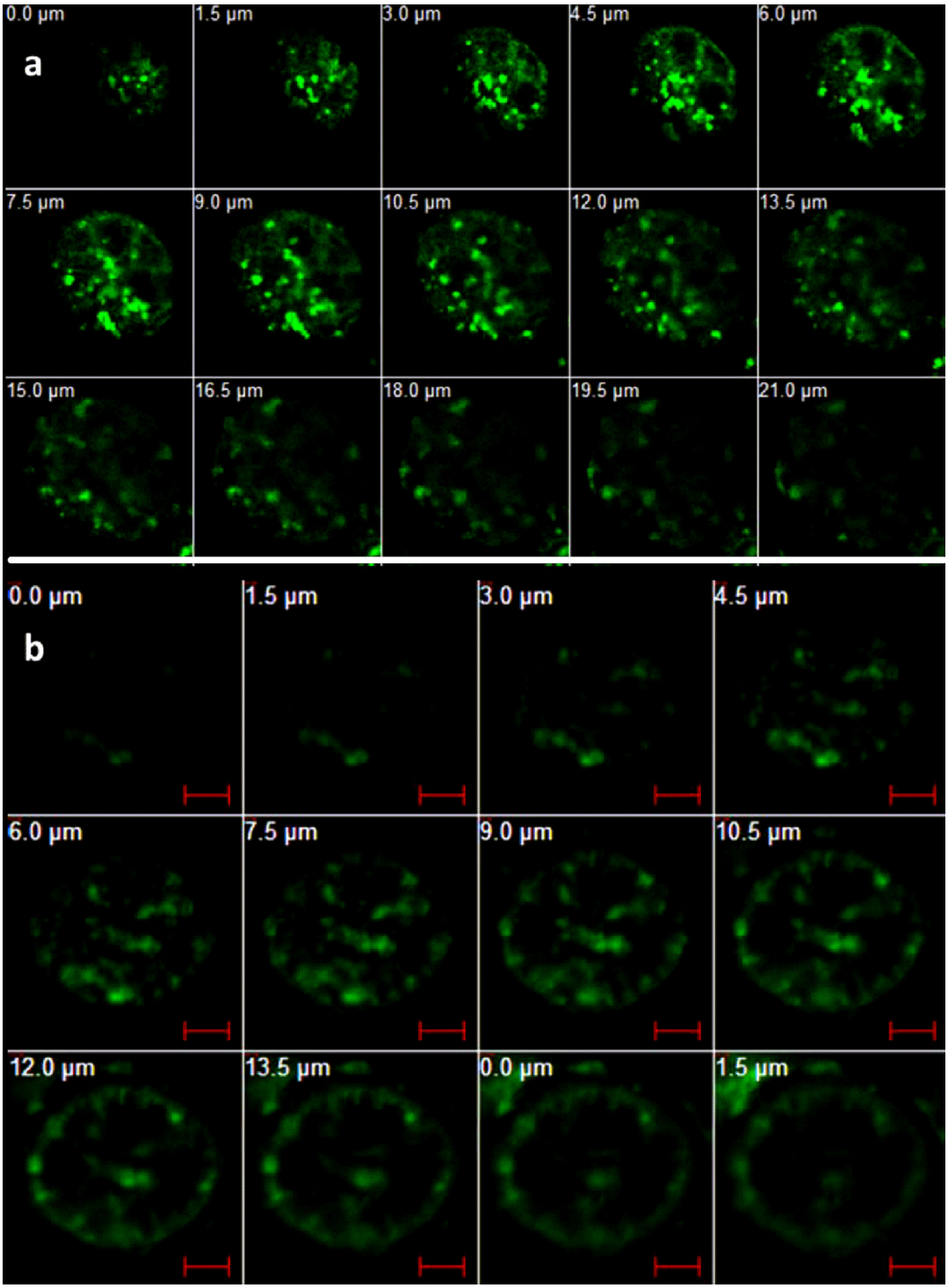

Fig. 4 – Confocal stacking images for I-FITC loaded in (A) PLGA MPs and (B) CS-PLGA MPs, CS concentration is 5 mg/ml.

surface of PLGA MPs at different CS concentrations compared to uncoated ones. SEM images reveal the disappearance of surface pores with the deposition of CS coating. By visual inspection and surface porosity data (Fig. 1E), it can be noted that the number of surface pores was inversely related to the CS concentration. Hence, CS concentration of 5 mg/ml showed the most efficient blocking (surface porosity decreased from 15% ± 6% to 1.3% ± 0.02%, $P < 0.001$) compared to the higher concentrations 10 and 15 mg/ml (surface porosity was 2.9% ± 1.3% and 6.6% ± 4% respectively, $P < 0.001$, Table 4). These findings confirm the reason for the highest LC% achieved with 5 mg/ml where the polymer diffusion into the pores towards the surface reached its maximum.

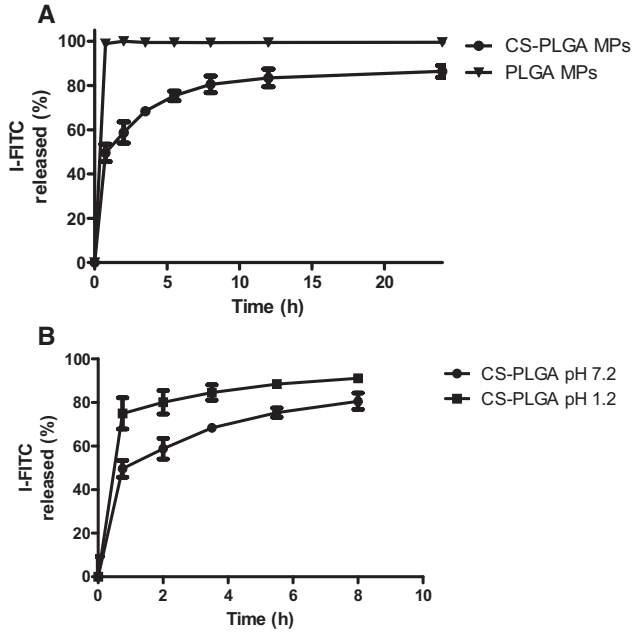

Fig. 5 – (A) I-FITC release profile from uncoated and coated PLGA MPs in phosphate buffer pH 7.2 at 37 °C, (B) I-FITC release profile from CS-PLGA MPs concentration 5 mg/ml in phosphate buffer pH 7.2 and potassium chloride buffer pH 1.2 at 37 °C. All samples were diluted and measured in pH 7.2.

3.5. *Studying the distribution of insulin among MPs after CS coating*

In order to detect the insulin distribution among porous MPs after CS coating, I-FITC loaded MPs were coated by CS using double freeze-drying and visualized by confocal microscope (Fig. 4). Confocal microscopy is an extensively used technique for the visualization of fluorescently labeled proteins and peptide molecules inside porous MPs [25,44]. When CS coating was introduced to PLGA MP surface (Fig. 4B), the fluorescence intensity was homogenously distributed among CS outer coat of the MPs compared to the fluorescent foci observed in uncoated counterparts indicating the presence of insulin molecules within CS coat (Fig. 4A). In addition, the interior matrix of the MPs also showed fluorescence within the porous matrix that persisted in deeper sections, however, the fluorescent intensity remains higher on the particle outer layers when compared to the MP core indicating the difficulty of insulin penetration to deeper layers.

3.6. *In vitro release of I-FITC from coated MPs*

Fig. 5 A shows a significant ($P < 0.001$) decrease in the burst release of I-FITC from the coated PLGA MPs when compared to the uncoated MPs. In the first hour about 49.6% ± 3.9% of I-FITC was released whereas almost all insulin was released at the same time interval from the uncoated MPs. However, despite the pore blocking by CS coating, premature release could still be observed. This can be explained by the physical adsorption of some I-FITC molecules on the surface of the polymer-shell around the MPs that remained even after the washing step. This proves the ability of CS coating to sustain the release of insulin from PLGA MPs while maintaining a primary burst release phase necessary for providing a rapid onset for insulin therapy.

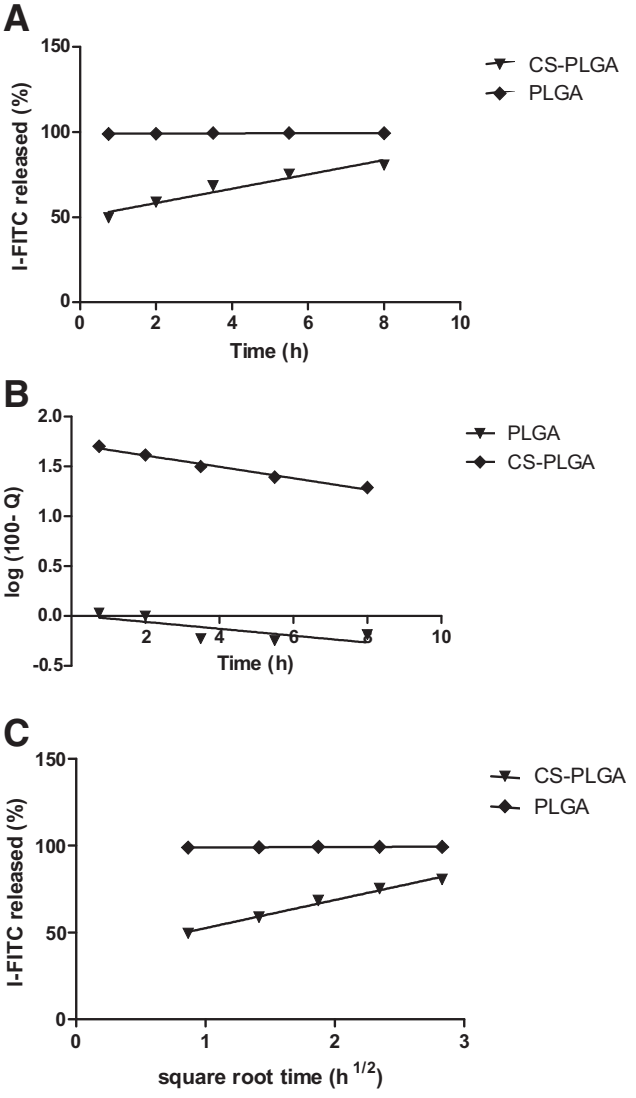

Fig. 6 – Release kinetics plots for I-FITC from CS coated and uncoated PLGA MPs (A) zero order, (B) first order and (C) Higushi.

Because of the significant effect of coating on I-FITC release from PLGA and due to CS pH sensitivity [45], we studied the pH variations in the GIT where MPs will be subjected to different environments that may affect their desorption, the release behavior of CS coated PLGA MPs was studied at two different pH values (1.2 and 7.2) at 37 °C to simulate gastric and intestinal pH respectively. Fig. 5B shows a two folds higher release of I-FITC at pH 1.2 in the first 2 h in comparison to pH 7.2. However, the release at pH 1.2 was still 1.5 folds lower than the release of uncoated MPs at pH 7.2. Moreover, the release pattern of insulin at pH 1.2 following the first 2 h was similar to that at pH 7.2. The slower release pattern following the first 2 h can be attributed to the CS adsorbed inside the pores that remained after swelling of the surface CS layers and slowed

Table 5 – The I-FITC release kinetic parameters from PLGA and CS coated PLGA MPs.

			PLGA	CS-PLGA
Kinetic model	Zero order	K_0	0.06 ± 0.03	4.2 ± 0.6
		R^2	0.6012	0.9347
	First order	K_1	−0.03 ± 0.01	−0.06 ± 0.004
		R^2	0.5706	0.9831
	Higushi	K	0.26 ± 0.1	16.2 ± 1
		R^2	0.7074	0.988

Data is represented as mean ± SD, n = 3.

down insulin release. It is to be noted that amine groups on glucosamine moieties of CS chain are protonated at pH lower than its pKa (approximately 6.8) hence the coat swelling increases and the flow of the release medium through the CS coat to dissolve I-FITC becomes much faster [45]. In addition, the lower pH value increases the protonation of insulin and subsequently its solubility.

To determine the release kinetics, the cumulative release was examined in different release models; zero order (4), first order (5) and diffusion controlled release (Higushi equation) (6)

$$Q = k^{\circ}t \tag{4}$$

$$\ln(100 - Q) = \ln Q^{\circ} - k1\,t \tag{5}$$

$$Q = kt^{1/2} \tag{6}$$

where Q is the % cumulative drug release at time t, k is the drug release constant.

From the coefficient of determination (R^2) for kinetic plots in Fig. 6A–C, it's apparent that the release of I-FITC from CS coated PLGA in the first 8 h fits best in the Higushi equation which indicates that the release mode is diffusion controlled (Table 5). This finding agrees with Bhattacharyya et al., [17] and Hao et al., [46] who examined the release from porous systems such as mesoporous silica and porous PLGA respectively. This proved that drug release from porous substrates is usually diffusion controlled, where liquid diffuses inside the pores and solubilizes the drug to be released. The release from CS based systems was also reported to be diffusion dependent [47], hence, the CS coating just slowed down the diffusion process rather than affecting the release kinetics. Although the R^2 in case of uncoated MPs was much lower than that of coated MPs, it still fitted the Higushi equation best. This linearity deviation would be due to the high initial burst achieved by the high porosity of the MPs. PLGA MPs possess large interconnected macropores which allowed large amounts of release medium to enter the particles in a short time and thus the release of the drug-dye conjugate occurred rapidly. In order to confirm the predominance of diffusion over polymer erosion in insulin release from both formulae; Kopcha equation was applied.

$$Q = At^{1/2} - Bt \tag{7}$$

where A and B are the diffusion and erosion terms respectively. When $A/B > 1$, diffusion prevails and vice versa [47], in our case, A/B is 3.85 and 4 for CS-PLGA and uncoated PLGA respectively indicating that diffusion prevails in the examined release portion.

3.7. *Determination of insulin structural integrity*

Both coated and uncoated MPs were suspended in 0.1 M HCl and the extracted insulin samples were run against standard insulin in SDS-PAGE. In Fig. 7A, the bands of all the tested samples appeared nearly at the same distance as that of standard insulin parallel to a 5 kDa molecular marker which is equivalent in Mwt to insulin hexamer. The bands were intact with no streaking and there weren't any signs of bands of smaller size suggesting the absence of any fragmentations in insulin structure. There were also no bands at earlier distance which represent larger size confirming the absence of any aggregates.

Fluorescent spectroscopy was also used to detect changes in insulin tertiary structure. This technique depends on the fluorescence of the four tyrosine residues in insulin structure at 307 nm [48,49]. The fluorescence maxima for insulin samples in 0.01 M HCl were measured and compared to that of standard insulin as well as denatured insulin. Fig. 7B shows the fluorescence spectra of insulin released from selected uncoated and CS coated PLGA formulae versus standard native insulin. All spectrofluorimetric spectra for insulin from different formulations had the same emission maxima at 307 nm compared to that of the denatured peptide which appeared at 332 nm, suggesting the absence of any structural changes of insulin released from the selected formulae. The preservation of insulin released from all formulae compared to native insulin confirms the intact conformation of the released insulin and hence the maintenance of its activity after loading. On the other hand, the red shift of the emission maximum from 307 to 332 nm that appeared with the denatured insulin suggests peptide unfolding and potentially the increased exposure of tyrosine [50]. Hence, we can conclude from *in vitro* data that the insulin released from both coated and uncoated formulae retains its size and tertiary structure.

3.8. *Pharmacological activity of insulin loaded on MPs*

For further assessment of the protecting effect of MPs on insulin integrity in the GIT, both coated and uncoated formulae were administered to rats then blood glucose was measured at several time intervals and the percent blood glucose reduction was calculated in comparison with SC and oral insulin suspensions. As shown in Fig. 8, insulin suspension administered orally showed no reduction in blood sugar due to the physical and chemical barriers against macromolecule absorption that occurs in the GIT [7]. In contrast, SC administration resulted in a rapid decrease in blood glucose levels reaching 15.8% ± 4% in the first hour and lasted for only 2 h before it rose again. Therefore, at least 2 daily injections are required for maintaining normal insulin level for diabetic patients [35]. As for all oral formulae, they proved to be significantly effective ($P < 0.001$) in reducing blood sugar relative to oral suspension reaching a reduction level of 47.9% ± 2% from coated PLGA. Although, the coated formula didn't significantly ($P > 0.05$) differ in the

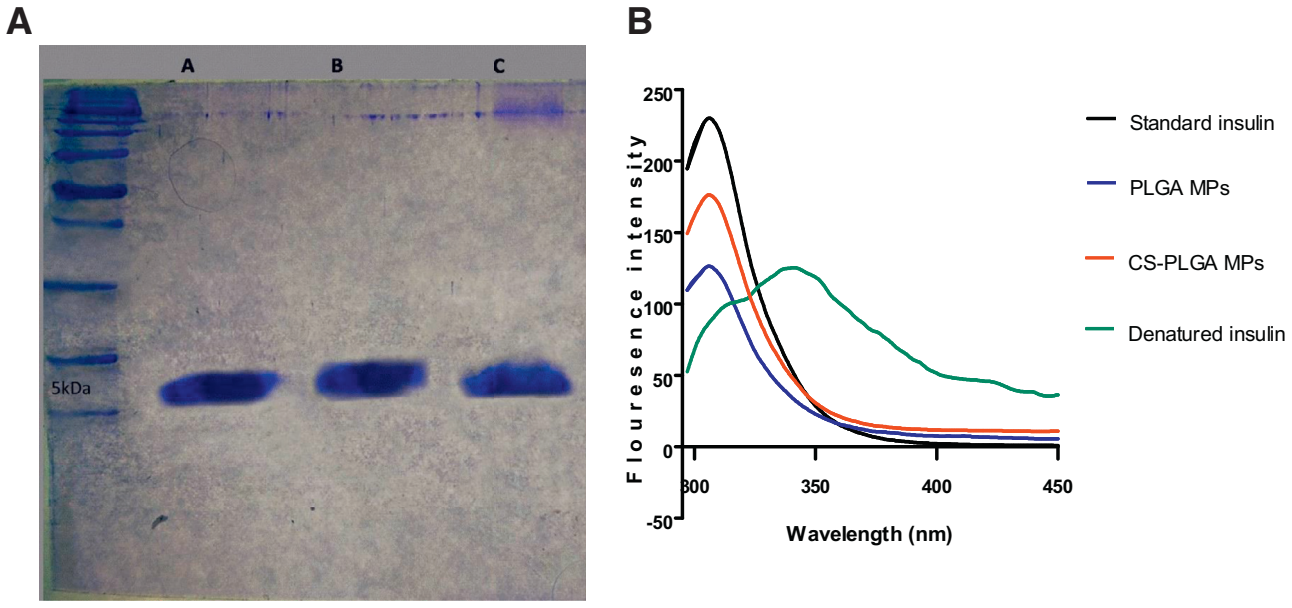

Fig. 7 – (A) SDS-PAGE analysis of lane A standard insulin, lane B insulin released from PLGA MPs loaded by freeze-drying, lane C insulin released from CS-PLGA loaded by double freeze-drying. (B) Fluorescence spectra of insulin released from both coated and uncoated PLGA MPs compared to standard and denatured insulin.

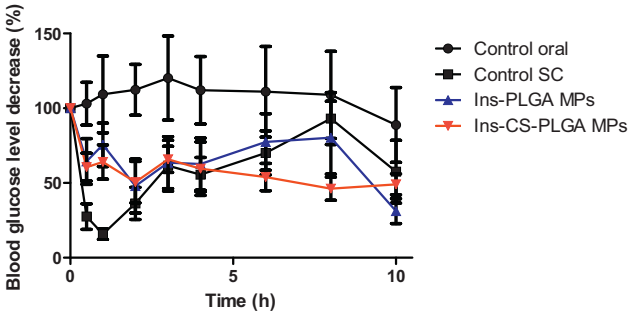

Fig. 8 – Blood glucose reduction profile after oral administration of insulin (ins) suspension, insulin loaded PLGA MPs, insulin loaded CS-PLGA MPs (50 IU/kg) and SC insulin suspension (5 IU/kg) (mean ± SE, N = 5).

magnitude of glucose reduction from uncoated counterpart, it increased the duration of action to over 8 h compared to uncoated preparation which lasted for only 4 h, indicating the sustained effect induced by CS coating. Despite the fact that the *in vitro* data showed faster release from CS coated PLGA particles at low pH simulating gastric acidity, the *in vivo* data still showed a sustained blood glucose reduction indicating a long residence time for the MPs in the GIT. This difference may be due to the fact that the MPs are administered as oral suspension which can pass the stomach of fasted rats rapid enough before CS could be dissolved at the gastric pH hence insulin loaded MPs can adhere to the upper intestinal wall (pH 5.5–6.5) where it would most likely be absorbed via insulin receptors on the enterocytes present in this region [51]. The sustained effect observed after oral administration can be attributed to the mucoadhesive action of CS along the absorption sites in GIT where CS adsorption to mucin is optimum. It is reported that mucin lining the GIT has an isoelectric point of 3 meaning that it's positively charged in stomach pH 1.2 and negatively charged in upper intestinal pH (above 5.5) [33]. Accordingly, despite the high protonation of CS in low pH, mucoadhesion is minimal while it's strong in that of upper intestine. For this reason, we can observe a sustained blood glucose lowering for the CS coated MPs. Similarly, many researchers were able to prove the sustained oral glucose reduction effect caused by CS coating of PLGA nanoparticles [5,52]. The second hypothesis would be that CS opens temporarily the tight junctions of the epithelial cells lining the GIT thus placing more insulin at the absorption site [34]. In addition, the higher insulin loading caused by CS coating also increased the amount of intact insulin remaining in contact with GIT mucosa for a longer time interval. Moreover, the small insulin absorption window occurs at the upper intestine pH (5.5–6.8) where the solubility of insulin is minimum [53], this offered slower release and maximum absorption from the CS muco-adhered MPs. From the pharmacodynamic data, coated MPs showed biphasic pattern in which blood sugar rises slightly to 70% after the first hour before decreasing again to maintain about 50% blood glucose reduction for 8 h. The reason for this may be due to surface insulin released from CS coat followed by the subsequent release from the pores. A similar pattern was observed from the uncoated PLGA MPs because of the high initial burst release associated with PLGA MPs due to weak interaction between insulin and PLGA.

From AAC measurements (Table 6), the BA_{rel} showed a remarkable increase by coating of PLGA reaching 11.52% when compared to 7.34% for uncoated MPs counterparts. The rise in BA_{rel} is due to the high loading capacity and protection ability achieved by CS coating. Accordingly, *in vivo* experiments con-

Table 6 – Pharmacodynamic parameters of glucose reduction upon SC and oral administration of insulin formulations to diabetic rats.

	Insulin administered SC	Insulin administered orally		
		Oral suspension	PLGA uncoated	CS-coated PLGA
Dose (IU/KG)	5	50	50	50
*T_{max} (h)	0.85 ± 0.1	——	1.5 ± 0.2	1.7 ± 0.3
*Max response	15.8	——	47.9 ± 18	50.6 ± 14
AAC	341.2 ± 26.3	81.8 ± 27.2	254.7 ± 51.8	383.4 ± 26.3
BAV (%)	100 ± 0	2.5 ± 1.3	7.3 ± 1	11.5 ± 2.76

*T_{max} *was calculated as time when the lowest blood glucose level was achieved, while the lowest magnitude of blood glucose reduction was denoted by Max response. Data is represented as mean ± SE. (n = 5).*

firmed the preservation of insulin activity both after loading and absorption from the GIT from the selected formulae.

4. Conclusion

We represent in this article for the first time the use of double freeze-drying as a novel technique for introducing a chitosan coating layer to block the surface pores of insulin loaded PLGA MPs and increase the loading capacity in the same time. The loading data proved that the new method could dramatically increase the amount of insulin loaded on the MPs. The LC% was dramatically increased to 20% and this makes it the highest reported loading capacity for a protein cargo into porous polymeric MPs among the recently published literature [16,28]. The LC% depended on both CS concentration and Mwt in an inverse relation after threshold concentration of 5 mg/ml. In addition, the insulin structural integrity was intact after loading as proved by SDS-PAGE and fluorescent spectroscopy. Furthermore, the release from coated MPs was more sustained and the oral BAV reached 11.52% for CS coated porous PLGA. Finally, pharmacodynamic *in vivo* studies of CS coated porous PLGA MPs using double freeze-drying technique has proved that these systems can be effective in the oral administration of macromolecules. However, further studies are still recommended to investigate insulin biodistribution and adjust the oral dosage regimen.

Declaration of interest

The authors report no conflicts of interest. The authors alone are responsible for the content and writing of this article.

Acknowledgment

We would like to thank SEDICO pharmaceutical company for kindly supplying the peptide and PURAC biomaterials for supplying PLGA polymers as a kind gift.

REFERENCES

[1] Uhlig T, Kyprianou T, Martinelli FG, et al. The emergence of peptides in the pharmaceutical business: from exploration to exploitation. Proteomics 2014;4:58–69.
[2] Gupta V. Glucagon-like peptide-1 analogues: an overview. Indian J Endocrinol Metab 2013;17:413–21.
[3] Ungaro F, d'Emmanuele di Villa Bianca R, Giovino C, et al. Insulin-loaded PLGA/cyclodextrin large porous particles with improved aerosolization properties: *in vivo* deposition and hypoglycaemic activity after delivery to rat lungs. J Control Release 2009;135:25–34.
[4] Al-Tabakha MM, Arida AI. Recent challenges in insulin delivery systems: a review. Indian J Pharm Sci 2008;70:278–86.
[5] Zhang X, Sun M, Zheng A, Cao D, Bi Y, Sun J. Preparation and characterization of insulin-loaded bioadhesive PLGA nanoparticles for oral administration. Eur J Pharm Sci 2012;45:632–8.
[6] Arbit E, Kidron M. Oral insulin: the rationale for this approach and current developments. J Diabetes Sci Technol 2009;3:562–7.
[7] Choonara BF, Choonara YE, Kumar P, Bijukumar D, du Toit LC, Pillay V. A review of advanced oral drug delivery technologies facilitating the protection and absorption of protein and peptide molecules. Biotechnol Adv 2014;32:1269–82.
[8] Ahmed RO. Pharmaceutical studies on pulmonary delivery systems of ciprofloxacin and DNaseI. Cairo: Ain Shams University; 2009.
[9] Manoharan C, Singh J. Addition of zinc improves the physical stability of insulin in the primary emulsification step of the poly(lactide-co-glycolide) microsphere preparation process. Polymers 2015;7:836.
[10] Yaghoobi N, Faridi Majidi R, Faramarzi Ma, Baharifar H, Amani A. Preparation, optimization and activity evaluation of PLGA/streptokinase nanoparticles using electrospray. Adv Pharm Bull 2017;7:131–9.
[11] Puri N, Jones AB, Kou JH, Wyandt CM. Release of bovine serum albumin from preformed porous microspheres of poly(L-lactic acid). J Microencapsulation 2000;17:207–14.
[12] Ungaro F, De Rosa G, Miro A, Quaglia F, La Rotonda MI. Cyclodextrins in the production of large porous particles: development of dry powders for the sustained release of insulin to the lungs. Eur J Pharm Sci 2006;28:423–32.
[13] Ahuja G, Pathak K. Porous carriers for controlled/modulated drug delivery. Indian J Pharm Sci 2009;71:599–607.
[14] Kim HK, Chung HJ, Park TG. Biodegradable polymeric microspheres with "open/closed" pores for sustained release of human growth hormone. J Control Release 2006;112:167–74.
[15] Reinhold SE, Desai K-GH, Zhang L, Olsen KF, Schwendeman SP. Self-healing microencapsulation of biomacromolecules without organic solvents. Angew Chem Int Ed 2012;51:10800–3.
[16] Bailey BA, Desai KH, Ochyl LJ, Ciotti SM, Moon JJ, Schwendeman SP. Self-encapsulating poly(lactic-co-glycolic acid) (PLGA) microspheres for intranasal vaccine delivery. Mol Pharm 2017;14:3228–337.
[17] Bhattacharyya S, Wang H, Ducheyne P. Polymer-coated mesoporous silica nanoparticles for the controlled release of macromolecules. Acta Biomater 2012;8:3429–35.
[18] Ganeshkumar M, Ponrasu T, Sathishkumar M, Suguna L. Preparation of amphiphilic hollow carbon nanosphere loaded insulin for oral delivery. Colloids Surf B Biointerfaces 2013;103:238–43.

[19] Li J, Jiang C, Lang X, et al. Multilayer sodium alginate beads with porous core containing chitosan based nanoparticles for oral delivery of anticancer drug. Int J Biol Macromol 2016;85:1–8.
[20] Wu J, Kong T, Yeung KWK, et al. Fabrication and characterization of monodisperse PLGA–alginate core–shell microspheres with monodisperse size and homogeneous shells for controlled drug release. Acta Biomater 2013;9:7410–19.
[21] Tang H, Guo J, Sun Y, Chang B, Ren Q, Yang W. Facile synthesis of pH sensitive polymer-coated mesoporous silica nanoparticles and their application in drug delivery. Int J Pharm 2011;421:388–96.
[22] Guo M, Rong WT, Hou J, et al. Mechanisms of chitosan-coated poly(lactic-co-glycolic acid) nanoparticles for improving oral absorption of 7-ethyl-10-hydroxycamptothecin. Nanotechnology 2013;24:245101.
[23] Belwalkar A, Grasing E, Van Geertruyden W, Huang Z, Misiolek WZ. Effect of processing parameters on pore structure and thickness of anodic aluminum oxide (AAO) tubular membranes. J Membr Sci 2008;319:192–8.
[24] Zhao W, Zhang H, He Q, et al. A glucose-responsive controlled release of insulin system based on enzyme multilayers-coated mesoporous silica particles. Chem Commun 2011;47:9459–61.
[25] Schlipf DM, Rankin SE, Knutson BL. Pore-size dependent protein adsorption and protection from proteolytic hydrolysis in tailored mesoporous silica particles. ACS Appl Mater Interfaces 2013;5:10111–17.
[26] Naha PC, Kanchan V, Manna PK, Panda AK. Improved bioavailability of orally delivered insulin using Eudragit-L30D coated PLGA microparticles. J Microencapsulation 2008;25:248–56.
[27] Hurkat P, Jain A, Shilpi S, Gulbake A, Jain S. Concanavalin A conjugated biodegradable nanoparticles for oral insulin delivery. J Nanopart Res 2012;14:1–14.
[28] Ansary R, Rahman M, Mohamad N, et al. Controlled release of lysozyme from double-walled poly(lactide-co-glycolide) (PLGA) microspheres. Polymers 2017;9:485.
[29] Guo C, Gemeinhart RA. Understanding the adsorption mechanism of chitosan onto poly(lactide-co-glycolide) particles. Eur J Pharm Biopharm 2008;70:597–604.
[30] Ahmed AR, Bodmeier R. Preparation of preformed porous PLGA microparticles and antisense oligonucleotides loading. Eur J Pharm Biopharm 2009;71:264–70.
[31] Kurata N, Anada S, Kawaguchi M. Competitive adsorption of polymer chains at fractal surfaces. In: Motoyuki S, editor. Studies in surface science and catalysis, Vol. 80. Elsevier; 1993. p. 341–8.
[32] Sonaje K, Chuang EY, Lin KJ, et al. Opening of epithelial tight junctions and enhancement of paracellular permeation by chitosan: microscopic, ultrastructural, and computed-tomographic observations. Mol Pharm 2012;9:1271–9.
[33] He P, Davis SS, Illum L. *In vitro* evaluation of the mucoadhesive properties of chitosan microspheres. Int J Pharm 1998;166:75–88.
[34] Pan Y, Li YJ, Zhao HY, et al. Bioadhesive polysaccharide in protein delivery system: chitosan nanoparticles improve the intestinal absorption of insulin *in vivo*. Int J Pharm 2002;249:139–47.
[35] Sonia TA, Sharma CP. An overview of natural polymers for oral insulin delivery. Drug Discovery Today 2012;17:784–92.
[36] Chen MM, Cao H, Liu YY, et al. Sequential delivery of chlorhexidine acetate and bFGF from PLGA-glycol chitosan core-shell microspheres. Colloids Surf B Biointerfaces 2017;151:189–95.
[37] Manca ML, Mourtas S, Dracopoulos V, Fadda AM, Antimisiaris SG. PLGA, chitosan or chitosan-coated PLGA microparticles for alveolar delivery? a comparative study of particle stability during nebulization. Colloids Surf B Biointerfaces 2008;62:220–31.
[38] Pastor E, Matveeva E, Valle-Gallego A, Goycoolea FM, Garcia-Fuentes M. Protein delivery based on uncoated and chitosan-coated mesoporous silicon microparticles. Colloids Surf B Biointerfaces 2011;88:601–9.
[39] Jiang T, Singh B, Li HS, et al. Targeted oral delivery of BmpB vaccine using porous PLGA microparticles coated with M cell homing peptide-coupled chitosan. Biomaterial 2014;35:2365–73.
[40] Ashworth EN, Abeles FB. Freezing behavior of water in small pores and the possible role in the freezing of plant tissues. Plant Phys 1984;76:201–4.
[41] Tozuka Y, Sugiyama E, Takeuchi H. Release profile of insulin entrapped on mesoporous materials by freeze–thaw method. Int J Pharm 2010;386:172–7.
[42] Leonard F, Margulis-Goshen K, Liu X, Srinivasan S, Magdassi S, Godin B. Low pressure mediated enhancement of nanoparticle and macromolecule loading into porous silicon structures. Meso Biomater 2014;1(1). doi:10.2478/mesbi-2014-0002.
[43] Abdelbary A, Elnabarawy MA, Hassen DA, Taha AA. Inclusion and characterization of ketoprofen into different mesoporous silica nanoparticles using three loading methods. J Pharm Pharm Sci. 2014;6:183–91.
[44] Desai K-GH, Schwendeman SP. Active self-healing encapsulation of vaccine antigens in PLGA microspheres. J Control Release 2013;165:62–74.
[45] Deng Z, Zhen Z, Hu X, Wu S, Xu Z, Chu PK. Hollow chitosan–silica nanospheres as pH-sensitive targeted delivery carriers in breast cancer therapy. Biomaterial 2011;32:4976–86.
[46] Hao S, Wang Y, Wang B, Deng J, Zhu L, Cao Y. Formulation of porous poly(lactic-co-glycolic acid) microparticles by electrospray deposition method for controlled drug release. Mater Sci Eng C Mater Biol Appl 2014;39:113–19.
[47] Liu C, Desai KGH, Tang X, Chen X. Drug release kinetics of spray-dried chitosan microspheres. Drying Technol 2006;24:769–76.
[48] Amidi M, Pellikaan HC, de Boer AH, Crommelin DJA, Hennink WE, Jiskoot W. Preparation and physicochemical characterization of supercritically dried insulin-loaded microparticles for pulmonary delivery. Eur J Pharm Biopharm 2008;68:191–200.
[49] Yin R, Han J, Zhang J, Nie J. Glucose-responsive composite microparticles based on chitosan, concanavalin A and dextran for insulin delivery. Colloids Surf B Biointerfaces 2010;76:483–8.
[50] Ladokhin AS. Fluorescence spectroscopy in peptide and protein analysis. Encyclopedia of analytical chemistry. John Wiley & Sons, Ltd; 2006.
[51] Wu ZM, Ling L, Zhou LY, et al. Novel preparation of PLGA/HP55 nanoparticles for oral insulin delivery. Nanoscale Res Lett 2012;7:299.
[52] Makhlof A, Tozuka Y, Takeuchi H. Design and evaluation of novel pH-sensitive chitosan nanoparticles for oral insulin delivery. Eur J Pharm Sci 2011;42:445–51.
[53] Song L, Zhi ZL, Pickup JC. Nanolayer encapsulation of insulin-chitosan complexes improves efficiency of oral insulin delivery. Int J Nanomed 2014;9:2127–36.